

Substituent effects on fluorene-based linear supramolecular polymerization

Guang-Wei Zhang, Meng-Cheng Luo, Jia-Qi Lei, Tao-Tao Zhong, Ying Wei, Ling-Hai Xie & Wei Huang

To cite this article: Guang-Wei Zhang, Meng-Cheng Luo, Jia-Qi Lei, Tao-Tao Zhong, Ying Wei, Ling-Hai Xie & Wei Huang (2019): Substituent effects on fluorene-based linear supramolecular polymerization, *Supramolecular Chemistry*, DOI: [10.1080/10610278.2019.1609679](https://doi.org/10.1080/10610278.2019.1609679)

To link to this article: <https://doi.org/10.1080/10610278.2019.1609679>

 View supplementary material 

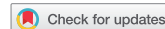
 Published online: 07 May 2019.

 Submit your article to this journal 

 Article views: 4

 View Crossmark data 

ARTICLE



Substituent effects on fluorene-based linear supramolecular polymerization

Guang-Wei Zhang^{*a}, Meng-Cheng Luo^{*a}, Jia-Qi Lei^a, Tao-Tao Zhong^a, Ying Wei^a, Ling-Hai Xie^a and Wei Huang^{a,b,c}

^aCenter for Molecular Systems & Organic Devices (CMSOD), Key Laboratory for Organic Electronics and Information Displays & Institute of Advanced Materials (IAM), Jiangsu National Synergetic Innovation Center for Advanced Materials (SICAM), Nanjing University of Posts & Telecommunications, Nanjing, China; ^bShaanxi Institute of Flexible Electronics (SIFE), Northwestern Polytechnical University (NPU), Xi'an, Shaanxi, China; ^cKey Laboratory of Flexible Electronics (KLOFE) & Institute of Advanced Materials (IAM), Jiangsu National Synergetic Innovation Center for Advanced Materials (SICAM), Nanjing Tech University (NanjingTech), Nanjing, China

ABSTRACT

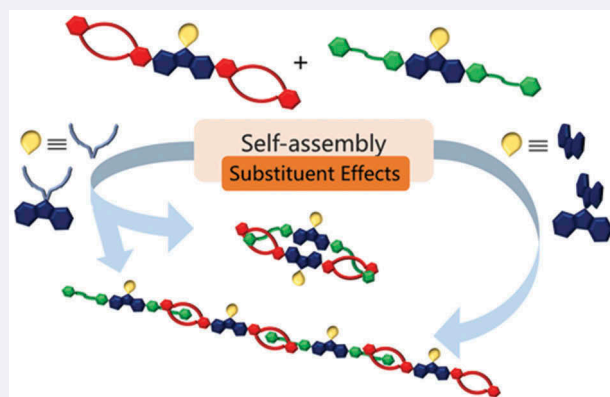
Two supramolecular systems were constructed based on fluorene-based π -conjugated monomers with or without spiro structures, respectively, and their self-assemble behaviour and optical properties were investigated. Concentration-dependent ^1H NMR and viscosity measurements indicated a transition from cyclic or oligomeric species at low concentrations to linear supramolecular polymers at high concentrations in the system without spiro structures. In contrast, the formation of cyclic species is minimised and not observed in the system with spiro structures.

ARTICLE HISTORY

Received 28 December 2018
Accepted 7 April 2019

KEYWORDS

Supramolecular polymer;
host-guest; fluorene;
substituent effects



Introduction

Supramolecular polymer materials combining the advantages of noncovalent bonds and covalent bonds have gained considerable interest in recent years (1–6). Supramolecular polymers with different topological structures offer a new way for creating novel supramolecular polymer species and functional materials (7), among which linear supramolecular polymers represent the most basic (simplest) type of extended noncovalent systems (8, 9), being direct counterparts of classical covalent polymers, and the research of them will help to further understand the basic construction principles of supramolecular polymers.

During the past several years, optoelectronic functional materials constructed by linear supramolecular polymers, have attracted considerable attention due

to their versatile applications in organic optoelectronic devices and chemical sensors (10–20). The optical and electronic functionalities in optoelectronic devices mainly derive from the intrinsic molecular structures of π -conjugated building blocks. Various π -conjugated units such as phenylene-ethynylene (PE) (21), tetraphenylethenes (22), fluorine (23–25), carbazole (12), thiophene (13) and their building blocks were introduced into optoelectronic supramolecular polymers to meet the requirements of organic devices. However, not so many examples were available with respect to introduce π -conjugated units into linear supramolecular polymers (15, 22–25), and a small part of them was about the introduction of fluorene-based π -conjugated units (23–25), which combine several advantageous properties that make them well-suited candidates for

CONTACT Wei Huang  iamdirector@fudan.edu.cn

*These authors contributed equally to the work.

 Supplemental data for this article can be accessed [here](#).

© 2019 Informa UK Limited, trading as Taylor & Francis Group

applications in organic optoelectronic devices (26). Herein, we designed fluorene-based linear supramolecular polymers by crown ether-based molecular recognition to study their supramolecular behaviour.

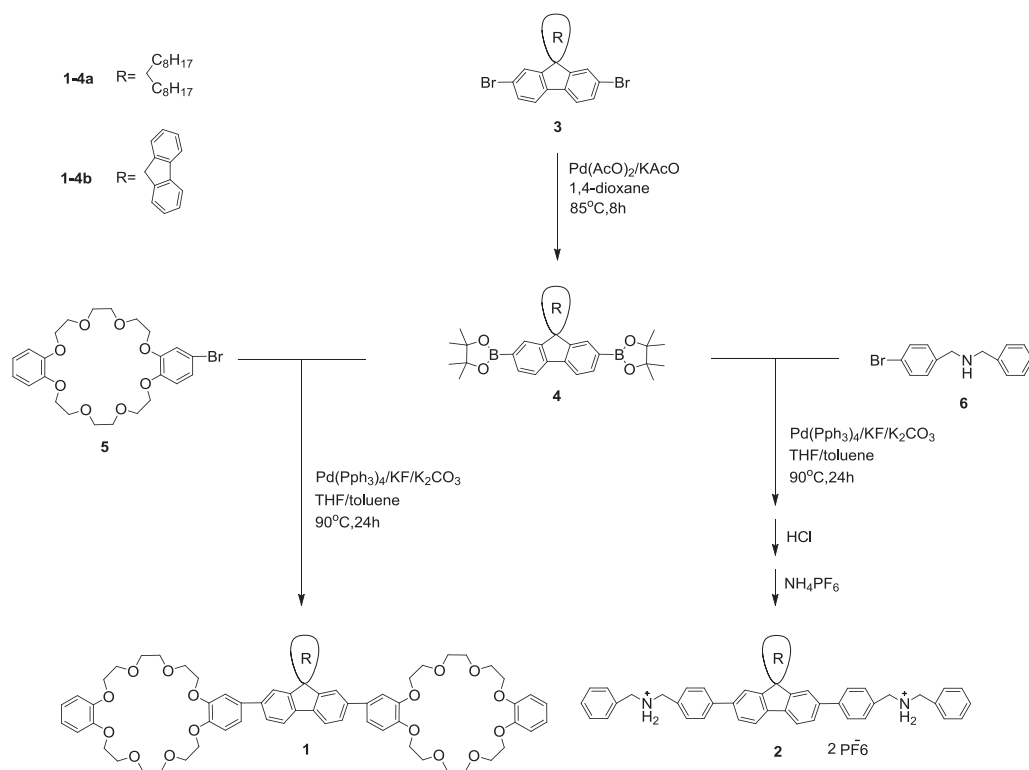
In our previous work (27), we proposed the strategy of hindrance functionalisation that incorporates of functional groups with steric hindrance effect into π -stacked polymers to tune their electronic structures, stacked conformations, morphological and thermal stability, and we investigated the substituent effects of bulky phenylfluorenyl moieties on the aggregate morphologies and device performances (28), and we found weak interchain interactions of the polymers in the solid state as a result of the steric hindrance of the spiro structures or bulky phenylene substituents. As far as we know, similar substituent effects on supramolecular polymers have been seldom reported (29–31). In this paper, bulky 9,9'-spirobifluorene (SBF) monomers were introduced into crown ether-based supramolecular systems, which were formed by utilising the efficient nonbonding self-assembly of luminescent SBF-based monomers, tethered with either a crown ether or dibenzylammonium unit. The secondary amines in the monomers are protonated and capable to be hosted by the crown ethers, thereby the host and the guest can self-assemble into supramolecular macromolecules via a host-guest

interaction. For comparison, the counterparts of non-spiro fluorene-based monomers were also researched, in which the fluorene ring connected to the backbone through a spiro-bridge was replaced by two alkyl chains, and thus the substituent effects of spiro structures were investigated (Scheme 1).

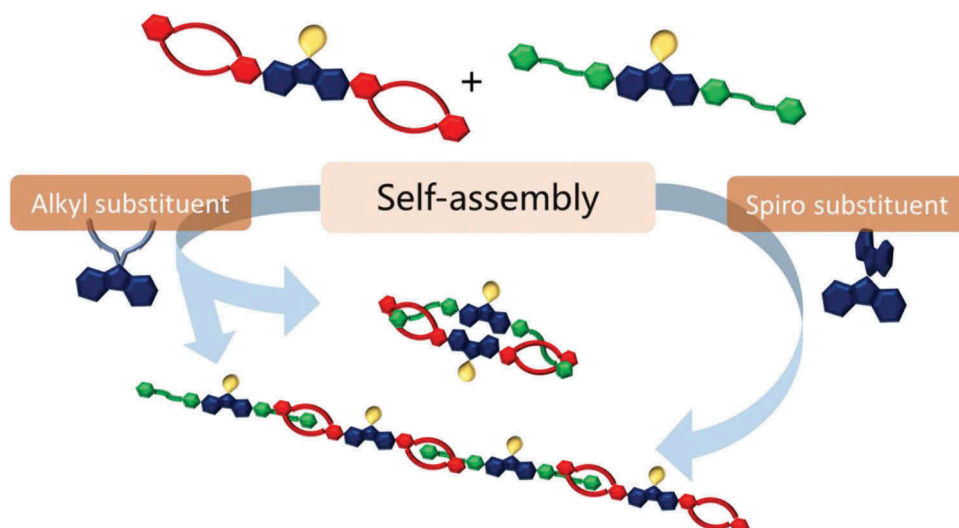
Results and discussion

Synthesis and characterisation

As shown in Scheme 2, the host monomers **1a** and **1b** were obtained by palladium-catalysed Suzuki cross-coupling reactions after the precursor compound **4a** and **4b** were synthesised. The guest monomers **2a** and **2b** were synthesised by a three-step procedure with a high yield (see supplementary material for details). Both compounds were fully characterised by ^1H NMR and ^{13}C NMR spectroscopy, as well as by Matrix-assisted laser desorption ionisation time-of-flight mass spectrometry. It is known that the association constant values of dibenzo-24-crown-8 (DB24C8) and dibenzylammonium hexafluorophosphate are desirably high ($K_a = 2.76 \times 10^4 \text{ M}^{-1}$ in D-chloroform at 25°C) (32, 33). Association of homoditopic monomers, that spontaneously form linear supramolecular polymers, is based on a pseudorotaxane



Scheme 1. Synthetic route to the monomers **1a**, **2a**, **1b** and **2b**.



Scheme 2. Cartoon representation of the formation of the supramolecular assemblies.

formation. The complexation behaviour of **1a** and **2a** in solution was investigated by ^1H nuclear magnetic resonance (NMR) studies. The concentration-dependent ^1H NMR spectra of an equimolar solution of **1a** and **2a** in $\text{CDCl}_3\text{-CF}_3\text{COOD}$ (3:1, v/v) at 25°C is shown in Figure 1. At high concentrations (above 20 mM), the benzyl protons have two sets of well-defined signals standing for the cyclic and linear species, respectively (34). The signals of the benzyl protons corresponding to the linear species at $\delta = 4.43$ ppm become more intense while the signals at $\delta = 4.72$ and 4.62 ppm corresponding to the cyclic species become less intense as the concentration is increased. The signals for the cyclic species appeared dramatically at 20 mM, and in addition, the signals are more intense, and the signals for the linear species are dominant below 20 mM. Similar to the complexation behaviour of **1a** and **2a**, the concentration-dependent ^1H NMR spectra of a 1:1 mixture of **1b** and **2b** in $\text{CDCl}_3\text{-CF}_3\text{COOD}$ (3:1, v/v) at 25°C in solution is shown in Figure 1. Only one set of signals of the benzyl protons is observed, which stand for the linear species, the signals at $\delta = 4.48$ ppm gradually move to $\delta = 4.65$ ppm and become more intense as the concentration is increased. At high concentrations, all signals become broad which confirms the formation of high-molecular-weight aggregates (35, 36). It is worth noting that the signals corresponding to cyclic species are too weak to be found in **SPb** system.

The morphologies of the monomers and their supramolecular systems were investigated by scanning electron microscope (SEM) images (as shown in Figure 2). These observations suggest that the twisted microscopic fibres with an average diameter of over $9.0\ \mu\text{m}$ were drawn from a low concentration solution of **1a:2a** (2 mM). The SEM images (Figure 2, Figure S23, S24) also

show that microscopic fibres with an average diameter over $1.0\ \mu\text{m}$ were complexed by **1b** and **2b** in a low concentration solution (2 mM). The observations of the fibres can provide indirect evidence for the formation of the supramolecular polymers.

Matrix-assisted laser desorption ionisation time-of-flight (MALDI-TOF) mass spectrometry can give intuitive information about the complexed behaviour of the host and the guest. MALDI-TOF-*ms* was employed to study the complexation behaviour of **1a** and **2a** (see Figure S19 in the Supporting Information). The resultant spectrum reveals the existence of the self-organised structure of **1a** and **2a**: m/z 2061.728, probably corresponding to $[\mathbf{1a}+\mathbf{2a}-2\text{H}-2\text{PF}_6^-]^+$ or $[n(\mathbf{1a}+\mathbf{2a}-2\text{H}-2\text{PF}_6^-)]^{n+}/n$. The other main peaks at 1304.814 and 780.575, corresponding to $[\mathbf{1a}+\text{Na}]^+$ and $[\mathbf{2a}-2\text{H}-2\text{PF}_6^-]^+$, respectively, are also observed. Similarly, the strong peaks at m/z 1916.316 for $[\mathbf{1b}+\mathbf{2b}-2\text{H}-2\text{PF}_6^-]^+$ or $[n(\mathbf{1b}+\mathbf{2b}-2\text{H}-2\text{PF}_6^-)]^{n+}/n$ and 1209.328 for $[\mathbf{1b}]^+$ are observed in MALDI-TOF-*ms* analysis of **1b** and **2b** (Figure S20). The MALDI-TOF-*ms* analysis could support the complexed behaviour of **1a** and **2a**, **1b** and **2b**.

The resonances of the host-guest complexes are assigned by means of 2D NMR experiments. The $^1\text{H}\text{-}^1\text{H}$ correlation spectroscopy ($^1\text{H}\text{-}^1\text{H}$ COSY) of 50 mM equimolar solution of **1a** and **2a** in $\text{CDCl}_3\text{-CF}_3\text{COOD}$ (3:1, v/v) at 25°C is shown in Figure S21 (see the Supporting Information). The cross peaks of $(\text{H}_{4\text{a}}, \text{H}_2)$, $(\text{H}_{4\text{a}}, \text{H}_3)$ show that **1a** and **2a** molecules interact strongly to form the host-guest complexes, and the diagonal peaks of (4.46 ppm, 4.46 ppm) (4.62 ppm, 4.62 ppm) and (4.72 ppm, 4.72 ppm) could be assigned as the complexed **2a**. Similar to the multicomponent assemblies shown by **1a** and **2a**, the $^1\text{H}\text{-}^1\text{H}$ COSY NMR

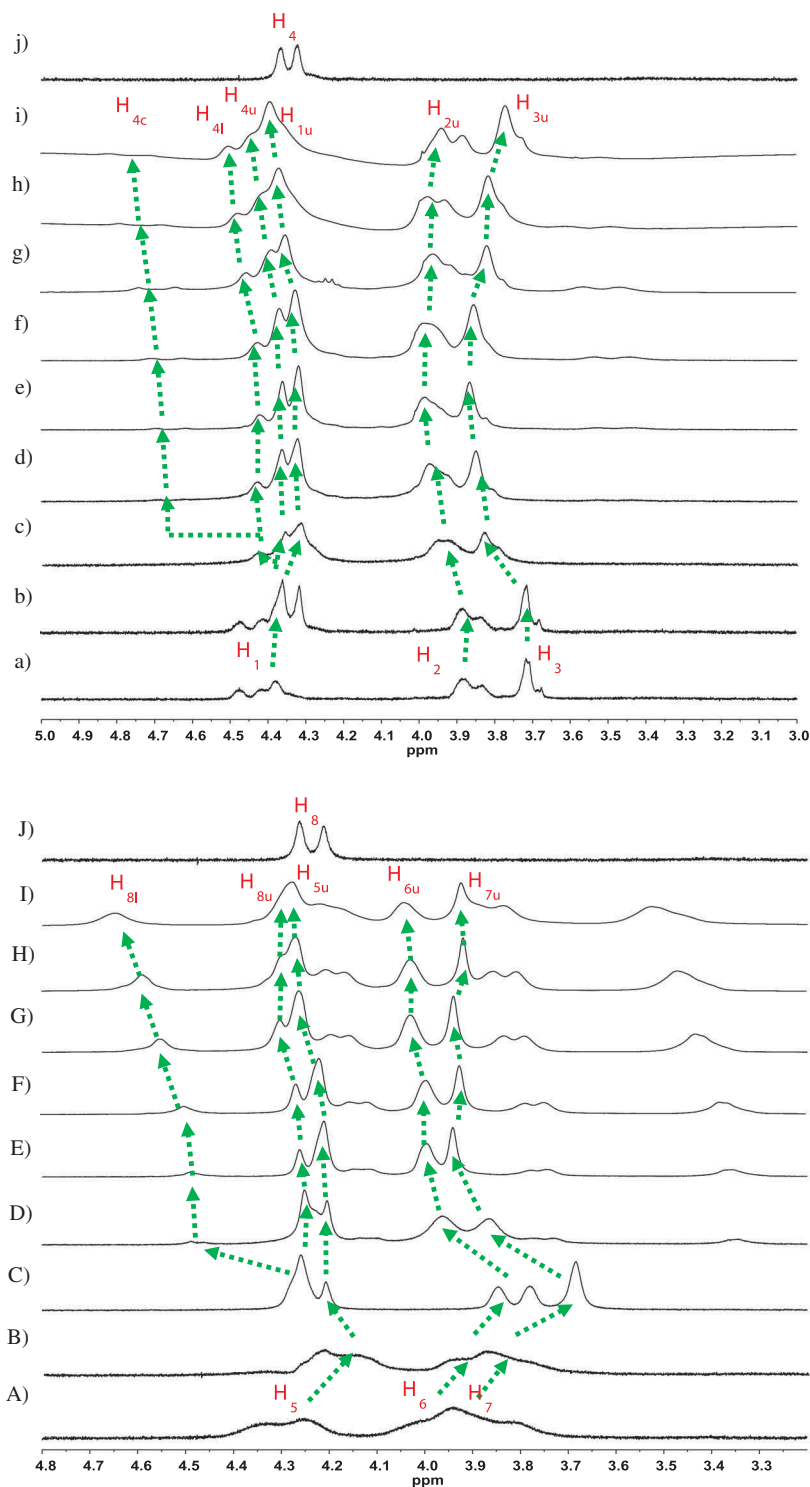


Figure 1. The stacked ^1H NMR spectra (400 MHz, $\text{CDCl}_3\text{-CF}_3\text{COOD}$ 3:1, v/v, 25°C) of solutions of **1a** and **2a** at different concentrations: (a) **1a**, (j) **2a**, and equimolar solutions with concentrations (b) 1, (c) 2, (d) 5, (e) 10, (f) 20, (g) 50, (h) 100, and (i) 200 mM; The stacked ^1H NMR spectra (400 MHz, $\text{CDCl}_3\text{-CF}_3\text{COOD}$ 3:1, v/v, 25°C) of solutions of **1b** and **2b** at different concentrations: (A) **1b**, (J) **2b**, and equimolar solutions with concentrations (B) 1, (C) 2, (D) 5, (E) 10, (F) 20, (G) 50, (H) 100, and (I) 200 mM. u: uncomplexed monomers, c: cyclic polymers, and l: linear supramolecular polymers.

experiments of **1b** and **2b** in the same conditions were carried out. The cross peaks of (H_8 , H_5), (H_8 , H_6), (H_8 , H_7) prove that **1b** and **2b** molecules interact strongly to form the host-guest complexes, and the diagonal peak

of (4.57 ppm, 4.57 ppm) can be assigned as the complexed **2b**. NOESY NMR techniques can be helpful to distinguish between linear species and cyclic species in supramolecular systems. The $^1\text{H}\text{-}^1\text{H}$ nuclear overhauser

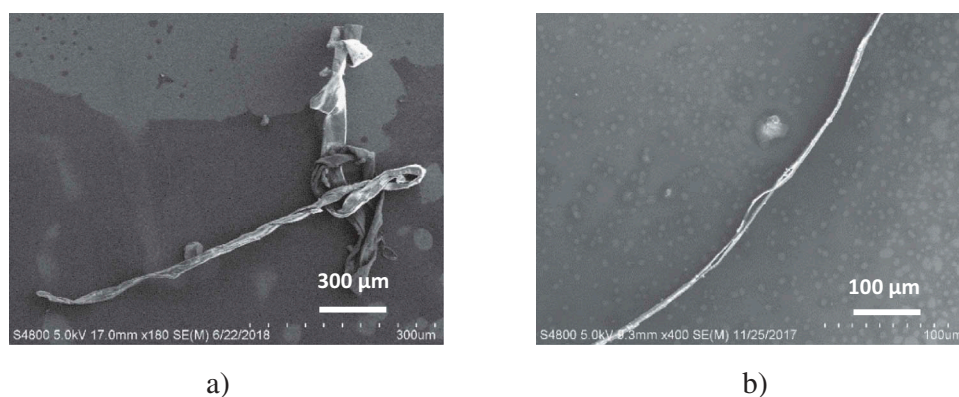


Figure 2. SEM images of the supramolecular systems: (a) **1a** and **2a**, (b) **1b** and **2b**.

effect spectroscopy (^1H - ^1H NOESY) of 50 mM equimolar solution of **1a** and **2a** in CDCl_3 - CF_3COOD (3:1, v/v) at 25°C is shown in Figure 3. It is found that three intermolecular cross-peaks between the protons of crown ether in **1a** and complexed proton H_4 in **2a**, which could be corresponding to the linear signal H_{4l} , and only one intermolecular cross-peak between the protons H_1 in **1a** and complexed proton H_4 in **2a** which could be corresponding to the cyclic signals H_{4c} in the ^1H - ^1H NOESY 2D NMR spectrum. It should be noted that the complexation behaviour of **1b/2b** is different from those of **1a/2a** in the ^1H - ^1H NOESY NMR in CDCl_3 - CF_3COOD (3:1, v/v) at 25°C (Figure 3a). There are five intermolecular cross-peaks between the complexed protons and uncomplexed protons of crown ether in **1b** and complexed proton H_8 in **2b**, which only can be corresponding to the linear signals H_{8l} . These results suggest that **1b** and **2b** favour the formation of linear polymers, not cyclic species. In other words, if the linkers in the ditopic monomers are spiro structures, the formation of cyclic species, a side reaction in the formation of supramolecular polymers, is minimised.

Due to the reversibility in the bonding, supramolecular polymers are often under thermodynamic control. Interaction of the host and guest moieties in these monomers is expected to produce cyclic and linear species, the ratio of which depends on a number of factors, including the concentrations and the nature of the linking groups. Generally, linear oligomers and polymers are in equilibrium with their cyclic counterparts, at low concentrations supramolecular polymers are known to exist preferably as cycles, whereas at higher concentrations linear polymers are formed (37). And by tuning the ratio of rigid units in the polymer chain on the basis of their reversibility, the ring-chain equilibrium of supramolecular polymerization can be controlled. Building blocks with more rigid spacer groups favour the formation of linear polymers, not cyclic oligomers (38, 39). For rigid polymers,

the probability of finding spacer ends within a bonding distance is smaller than for flexible polymers, which leads to a decrease in the total fraction of rings.

In this work, the spiro structure building blocks favour the formation of linear, not cyclic species which also can be considered as supramolecular steric hindrance effect as we early reported originating from the combination of the steric hindrance effect of rigid moieties with weak noncovalent interaction (40). It is conceivable that the rigid core with a spiro structure of **SPb** is bulky and rigid enough to suppress the dimerisation or cyclisation (Scheme 2). As a thermodynamic explanation, it can be believed that in this system linear species are more thermodynamically stable and favoured over cyclic ones due to lower Gibbs free energies, which is related to the introduction of spiro structures.

For direct physical evidence of the formation of large self-assembled noncovalent polymers, concentration-dependent viscosity measurements were investigated. A double logarithmic representation of specific viscosity versus the concentration of an equimolar solution of host and guest in CHCl_3 - CF_3COOH (3:1, v/v) is observed (as shown in Figure 4). For the **1a:2a** system, the slope of Figure 4a at low concentrations is 0.42, this is attributed to the presence of cyclic species. Interestingly, deviation from the line at low concentrations begins at 19 mM, indicating that large oligomers are already beginning to form. The slope at high concentrations, 1.99, is attributed to the formation of high molecular weight polymers. For the **1b:2b** system (Figure 4b), in the low concentration range, the curve has a slope of 0.62, which is characteristic for non-interacting assemblies of constant size. As the concentrations increase with a critical concentration about 20mM, the slope of the curve significantly increases to 2.16, indicating the dramatically increased viscosity due to the formation of the linear supramolecular polymers (high molecular

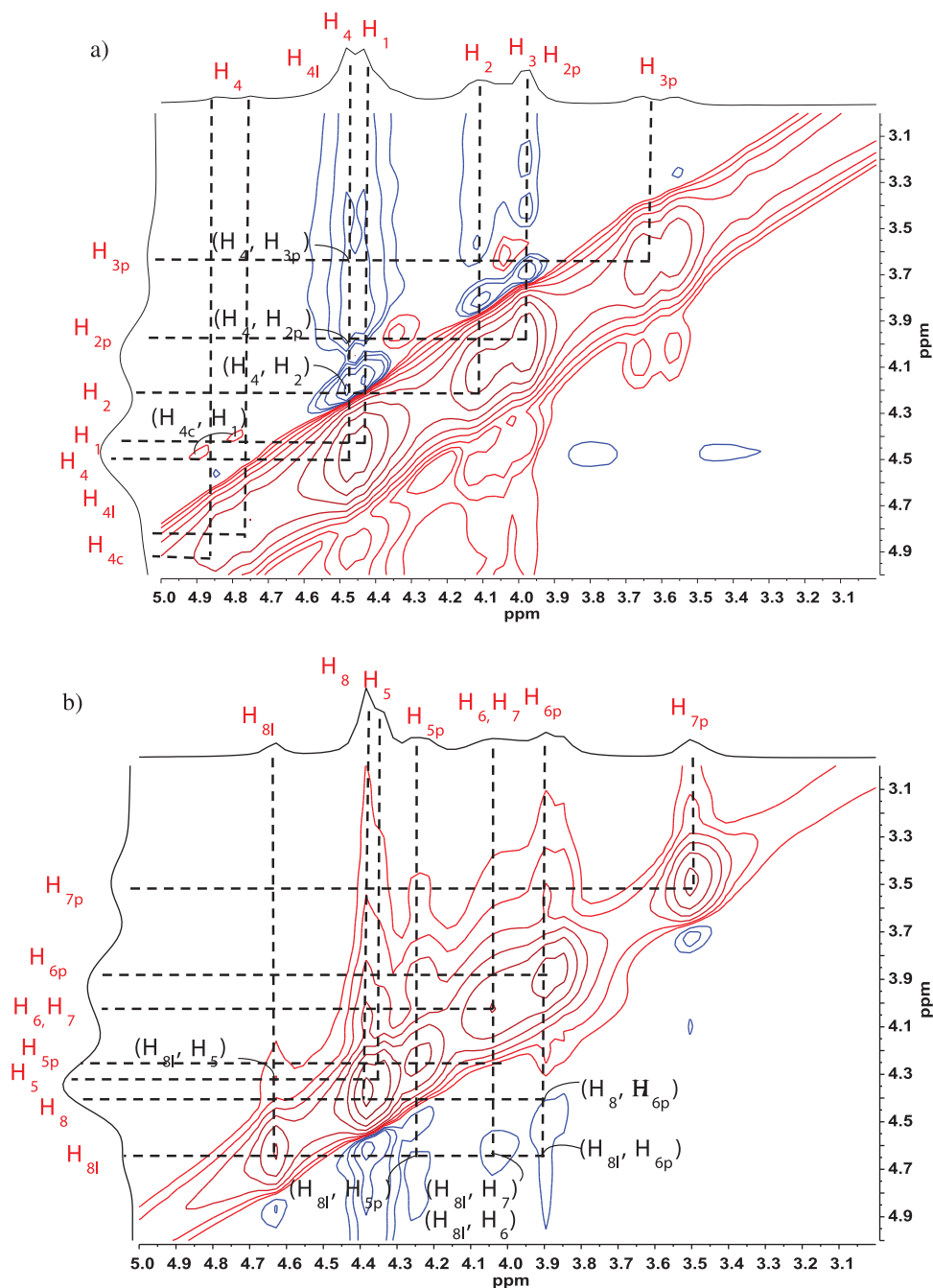


Figure 3. The ^1H - ^1H NOESY spectra (400 MHz, CDCl_3 - CF_3COOD 3:1, v/v) of 50 mM equimolar solution of (a) **1a** and **2a**. (b) **1b** and **2b**. p: complexed monomers, c: cyclic polymers, and l: linear supramolecular polymers.

weight polymers). All the results indicate a transition from cyclic or oligomeric species at low concentrations to linear polymers at high concentrations.

To further determine the formation of the linear supramolecular polymers **SPa** and **SPb**, the thermal behaviors of the supramolecular polymers **SPa** and **SPb** were investigated by differential scanning calorimetry (DSC) tests. As shown in Figure 4c and d, the DSC studies show that **SPa** has a distinct glass transition with a T_g of 95°C, which is substantially higher than those of **1a** (81°C) and **2a** (54°C),

and **SPb** with a T_g of 93°C substantially higher than those of **1b** (54°C) and **2b** (68°C), indicating the formation of the supramolecular polymers. It should be noted that the glass transition T_g of **SPa** is higher than that of **SPb**, which is in accordance with their association constant values of the host and guest. As shown in Figure S17 and S18, the association constant values of an 50 mM solution of **SPa** and **SPb** in CHCl_3 - CF_3COOH (3:1, v/v) at 25°C are $2.69 \times 10^3 \text{M}^{-1}$ and $0.96 \times 10^3 \text{M}^{-1}$ respectively, and the former is slightly higher than the later.

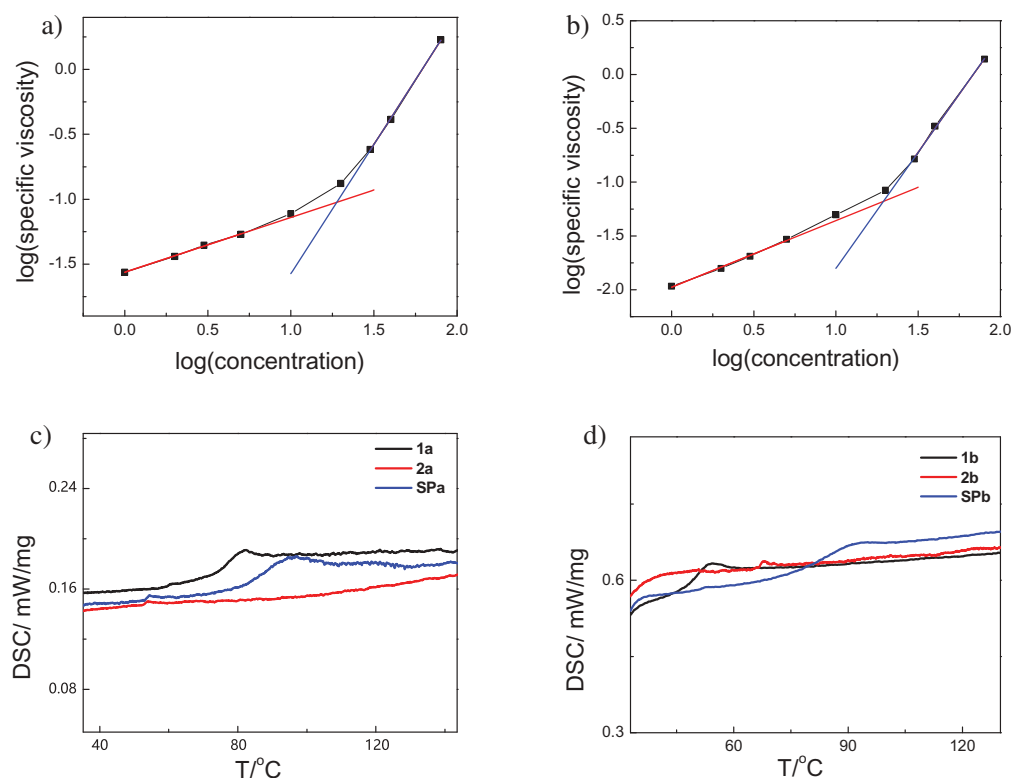


Figure 4. (a) Viscosity at different concentrations of **SPa**. (b) Viscosity at different concentrations of **SPb**. (c) DSC plots of host **1a**, guest **2a** and **SPa**. (d) DSC plots of host **1b**, guest **2b** and **SPb**.

UV–Vis absorption and fluorescence spectra of **1a**, **2a**, **SPa**, **1b**, **2b** and **SPb** were all measured in CHCl_3 – CF_3COOH (3:1, v/v) at different concentrations (Figure S25–S42). **1a** shows two absorption peaks at 240 nm and 333 nm, and a broad PL spectrum which contains two peaks at 378 nm and 392 nm with the onset at 500 nm. As the concentration increases, the absorption at 240 nm gradually increases and is stronger than the absorption peak at 333 nm. As shown in the PL spectrum, the fluorescence intensity increases with increasing concentrations at low concentrations, yet decreases with increasing concentrations at high concentrations, and the critical aggregation concentration is ca. 200 μM . **2a** shows two absorption peaks at 236 nm and 335 nm, and an emission maximum peak at 388 nm with a vibronic shoulder peak at 410 nm (Figure S28–S30), and an identifiable shoulder at around 550 nm with a long tail beyond 620 nm. The absorption at 335 nm gradually increases as the concentration increases, the critical concentration of PL is about 100 μM . **SPa** shows an absorption maximum peak at 334 nm and an emission maximum peak at 390 nm with a vibronic shoulder peak at 413 nm (Figure S31–S33). The absorption at 334 nm gradually increases as the concentration increases, and the critical concentration is ca. 200 μM , which is lower than that of the viscosity test, indicating that the monomer molecules have begun to

aggregate before the formation of the supramolecular polymers. **1b** exhibits an absorption maximum peak at 335 nm and an emission maximum peak at 387 nm with a vibronic shoulder peak at 410 nm. The optical images show that the absorption peak at 335 nm gradually increases as the concentration increases, the fluorescence peak at 387 nm gradually becomes more intense compared to the peak at 410 nm (Figure S34–S36), and the critical concentration is ca. 200 μM . **2b** exhibits three absorption peaks at 239 nm, 310 nm and 335 nm, and an emission maximum peak at 369 nm with a vibronic shoulder peak at 385 nm (Figure S37–S39), and an identifiable shoulder at around 500 nm with a long tail beyond 600 nm. When the concentration increases, the absorption peaks all gradually increase, the emission at 385 nm is gradually stronger than the emission at 369 nm, and the critical concentration is about 100 μM . **SPb** exhibits an absorption maximum peak at 336 nm and an emission maximum peak at 390 nm with a vibronic shoulder peak at 411 nm (Figure S40–S42). The absorption at 335 nm gradually increases as the concentration increases, and the critical concentration of PL is about 200 μM . It is worth noticing that each one of the PL spectra of **1b** and **2b** has a long tail extending to longer wavelength direction (the spectrum “onsets” at 620 nm at the longer wavelength side) and a shoulder at around 550 nm

(Figure 5c, d). This spectral feature is commonly observed in 9,9-disubstituted polyfluorenes and can be attributed to interchain excimers formation (41–44), which is proved by time-resolved fluorescence measurements (see Figure S43, S44 in the Supporting Information). In the region with long-wavelength fluorescence with a concentration at 10^{-4} mol/L, the mean fluorescence life-times are ca. 1.96 ns (for **2a** at 550 nm), and 1.86 ns (for **2b** at 500 nm) which are shortened to 0.86 ns (for **2a** at 390 nm) and 0.98 ns (for **2b** at 385 nm) in the region with short-wavelength fluorescence, respectively. The lengthening of the fluorescence life-times is very characteristic for excimer effects, in contrast to processes induced by the aggregation phenomenon, where distinct life-time shortening or decay is usually observed (45, 46). Compared with **2a** and **2b**, **SPa** and **SPb** show different PL spectra without apparent excimers or exciplexes peaks, and it can be understood that the hydrogen bonding interactions between the guest monomers are replaced by host-guest interactions between the hosts and the guests.

We also noted a marked difference among fluorescence spectra of them at different concentrations in the relative intensity of the emission bands, with the second (or shoulder) fluorescence band being more intense compared to the first (Figure S29, S30, S38, S39) as the concentration is increased. This might be ascribed to self-absorption phenomena due to the overlap of the 0–0

transition emission band and the absorption band which lead to a relative decrease of the intensity of the 0–0 transition (47). Above the critical concentration, all the systems present apparent concentration weakening of their fluorescence which is generally attributed to molecular aggregation. With an increase in the concentration, the probability of the formation of aggregates increases, thereby accentuating the self-absorption and thus the fluorescence weakening effect (48–50). The emission spectra of most aromatic compounds are concentration dependent. While at very low concentration fluorescence from monomer alone is observed, at higher concentrations emissions from both monomers and aggregates are observed. In general, fluorescence is often weakened or quenched at high concentrations due to a variety of interactions, such as radiative and non-radiative transfer and excimer formation. The latter two factors are typically a result of the formation of aggregates, and apparently in this work, the aggregates accentuating the self-absorption are most probably responsible for the non-radiative transfer and excimer formation.

Conclusions

In conclusion, conjugated monomers with or without spiro structures were introduced into two supramolecular systems, respectively, and their self-assemble behaviour and

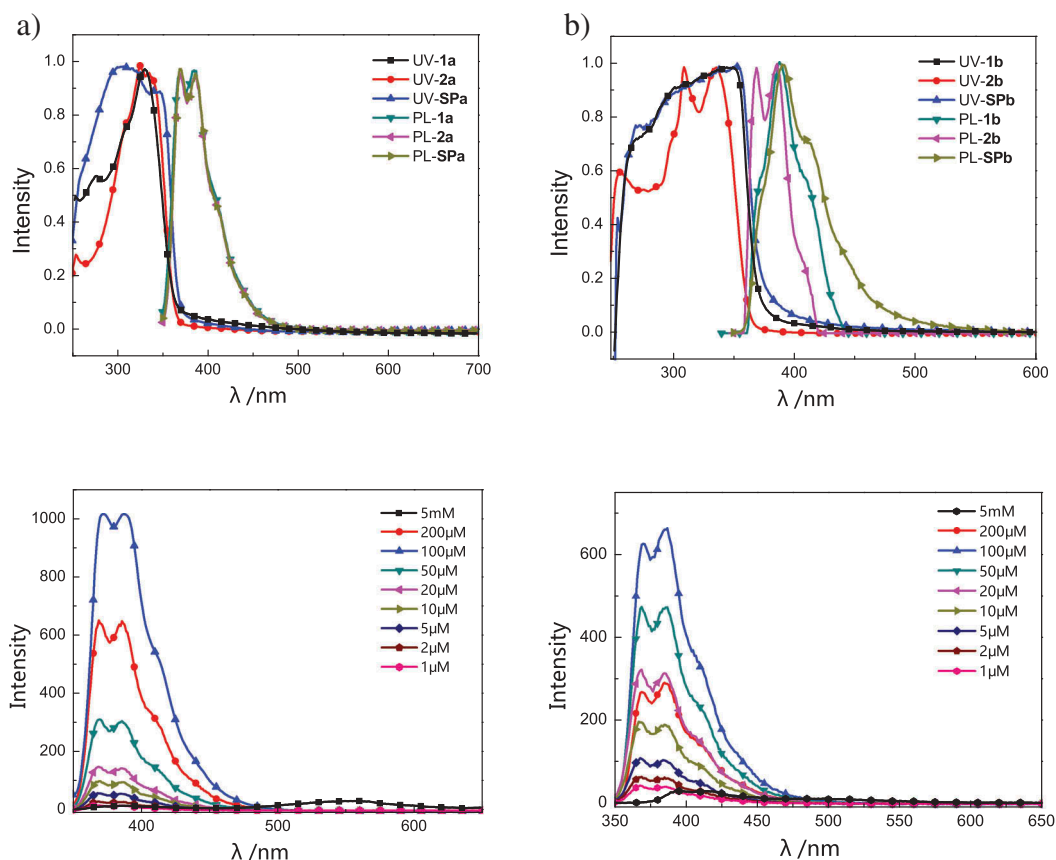


Figure 5. UV-visible absorption and PL spectra in CHCl_3 - CF_3COOH (3:1, v/v) solution of (a) host **1a**, guest **2a** and **SPa**. (b) host **1b**, guest **2b** and **SPb**. Fluorescence spectra of **2a** and **2b** (from 1 μ M increase to 5 mM) in CHCl_3 - CF_3COOH (3:1, v/v) solution of (c) **2a**. (d) **2b**.

intermolecular aggregation properties were investigated. The identity of the synthesised compounds was confirmed by NMR spectroscopy and mass spectral analysis. The supramolecular assembly processes were monitored and illustrated by concentration-dependent ^1H NMR, 2D NMR, SEM, DSC and viscosity measurements. The fluorescent results show that the assemblies display fluorescence weakening with the increase of concentration at high concentrations, and the formation of the excimers is found in the guests with protonated amine groups. The results suggest that the spiro structure building blocks probably favour the formation of linear supramolecular polymers, not cyclic species, which is most likely due to the substituent effects, and further study needs to be done to find the precise reasons leading to such different supramolecular polymerisation behaviour.

Experimental

Materials and methods

All reagents were obtained from commercial sources without further purification unless otherwise mentioned. The compounds of **4a**, **4b** were prepared according to the literature procedures (51, 52). NMR was recorded on a Bruker 400 MHz spectrometer using CDCl_3 , MeOD-d_4 , DMSO-d_6 and $\text{CDCl}_3\text{-CF}_3\text{COOD}$ (3:1, v/v) as solvents. MALDI-TOF mass spectra were taken on a Bruker BIFLEX III ultra-high resolution Fourier transform ion cyclotron resonance (FT-ICR) mass spectrometer with α -cyano-4-hydroxycinnamic acid as matrix. DSC measurements were acquired using a Shimadzu Instruments DSC-60A. DSC data were collected from 30°C to 210°C at a rate of 5°C/min for both of the baseline and sample. SEM images were obtained using a Hitachi S-4800 field-emission scanning electron microscopy. Specific viscosity was obtained using a Viscosimeter (0.5–0.6 mm). Absorption spectra (1 μM increase to 50 mM in $\text{CHCl}_3\text{-CF}_3\text{COOH}$, 3:1, v/v) were measured with a Shimadzu UV-3600 spectrometer at 25°C, and emission spectra (1 μM increase to 50 mM in $\text{CHCl}_3\text{-CF}_3\text{COOH}$, 3:1, v/v) were recorded on a Shimadzu RF-5301(PC) luminescence spectrometer. The fluorescence decay was measured using an Edinburgh FLSP920 fluorescence spectrophotometer equipped with a xenon arc lamp (Xe900).

Synthetic procedures

Synthesis of compounds 1a and 1b

2,2'-(9,9-dioctyl-9H-fluorene-2,7-diyl)bis(4,4,5,5-tetramethyl-1,3,2-dioxaborolane) (**4a**) (0.85 g, 1.5 mmol), 4-Bromo-dibenzo-24-crown-8 (1.62 g, 3.08 mmol),

and tetrakis(triphenylphosphine)palladium [$\text{Pd}(\text{PPh}_3)_4$] (110 mg) were added to a 100 mL two-necked round-bottomed flask. Toluene (10 mL), THF (10 mL), KF and K_2CO_3 each 1 mol/L hydroxide (3 mL) were added to the flask under nitrogen. The mixture was refluxed for 24 h under a nitrogen atmosphere. After the mixture had been cooled to room temperature, the mixture was poured into brine. Then, the mixture was extracted with dichloromethane, the two phases were separated, and the aqueous phase was extracted twice with dichloromethane. The combined organic extracts were washed three times with water, dried over MgSO_4 , evaporated, and purified with column chromatography (silica gel, ethyl acetate–dichloromethane (4/1) as eluent) to yield 670 mg (Yield: 37.0%) of **1a** as a light yellow semi-solid. ^1H NMR (400 MHz, Chloroform-*d*) δ 7.79–7.75 (d, J = 8.1 Hz, 2H), 7.57–7.53 (d, J = 7.5 Hz, 2H), 7.51 (s, 2H), 7.39–7.33 (d, J = 10.3 Hz, 4H), 7.20–7.16 (d, J = 8.2 Hz, 2H), 7.11–7.04 (m, 8H), 4.45–4.26 (m, 16H), 3.88–3.75 (m, 16H), 3.69–3.60 (m, 16H). ^{13}C NMR (400 MHz, Chloroform-*d*) δ 148.23, 137.16, 125.90, 123.63, 123.40, 122.27, 121.10, 120.20, 116.92, 116.54, 116.25, 115.75, 69.29, 69.04, 68.48, 68.25, 67.76, 67.62, 67.51, 67.31, 67.21, 55.41, 40.38, 31.77, 29.99, 29.71, 29.21, 23.87, 22.59, 14.09. MS (Madi-Tof): calcd $[\text{M}]^+$ 1282.717, $[\text{M}+\text{Na}]^+$ 1305.706, Found: $[\text{M}]^+$ 1282.672, $[\text{M}+\text{Na}]^+$ 1305.672, $[\text{M}+\text{K}]^+$ 1321.673.

The methods for preparing **1b** are the same. Yield: 30.4%. The proton NMR spectrum of **1b** is shown in Figure S6. ^1H NMR (400 MHz, Chloroform-*d*) δ 7.90–7.84 (d, J = 7.9 Hz, 4H), 7.56–7.52 (dd, J = 8.0, 1.6 Hz, 2H), 7.40–7.35 (t, J = 7.5 Hz, 2H), 7.14–7.09 (t, J = 7.5 Hz, 2H), 6.95 (s, 2H), 6.94–6.91 (d, J = 2.1 Hz, 2H), 6.89–6.84 (m, 8H), 6.84 (s, 2H), 6.83–6.77 (t, J = 8.4 Hz, 4H), 4.17–4.08 (m, 16H), 3.93–3.84 (dt, J = 8.5, 5.1 Hz, 16H), 3.83–3.77 (d, J = 3.4 Hz, 16H). ^{13}C NMR (400 MHz, Chloroform-*d*) δ 149.74, 148.92, 148.91, 148.88, 148.58, 140.46, 134.50, 127.90, 127.75, 126.60, 124.29, 122.26, 121.42, 120.23, 120.18, 120.07, 114.06, 113.98, 113.55, 71.24, 71.19, 69.91, 69.85, 69.76, 69.44, 69.37, 69.34, 29.72. MS (Madi-Tof): calcd $[\text{M}]^+$ 1208.513, $[\text{M}+\text{Na}]^+$ 1230.421. Found (%): $[\text{M}]^+$ 1207.411, $[\text{M}+\text{Na}]^+$ 1230.421, $[\text{M}+\text{K}]^+$ 1246.416.

Synthesis of compounds 2a and 2b

2,7-bis(4,4,5,5-tetramethyl-1,3,2-dioxaborolan-2-yl)-9,9'-spirobi[fluorene] (**5**) (1.42 g, 2.5 mmol), N-benzyl-1-(4-bromophenyl)methanamine (1.72 g, 6.25 mmol), and tetrakis(triphenylphosphine)palladium [$\text{Pd}(\text{PPh}_3)_4$] (180 mg) were added to a 100 mL two-necked round-bottomed flask. Toluene (15 mL), THF (15 mL), KF and K_2CO_3 each 1 mol/

L hydroxide (5 mL) were added to the flask under nitrogen. The mixture was refluxed for 24 h under a nitrogen atmosphere. After the mixture had been cooled to room temperature, pour dilute hydrochloric acid (0.5 M, 50 mL) into the mixture. Then, the mixture was extracted with dichloromethane, the two phases were separated, and the aqueous phase was extracted twice with dichloromethane. The combined organic extracts were filtered, and dichloromethane was removed with a rota evaporator. The solid was washed three times with 50 mL of ethyl acetate dried, the mixture was filtered and the solid was poured into water. The mixture was added to a saturated NH_4PF_6 solution to produce a precipitate. It was collected by suction filtration and recrystallised from deionised water three times to afford to yield 1.12 g (63.5%) of **2a** as a light grey semi-solid. ^1H NMR (400 MHz, Chloroform-*d*) δ 9.99 (s, 4H), 7.63 (s, 8H), 7.58 (s, 4H), 7.56 (s, 2H), 7.49 (s, 2H), 7.38 (s, 4H), 7.36 (s, 4H), 4.06–3.89 (d, *J* = 20.9 Hz, 8H), 1.96 (s, 4H), 1.17–1.10 (m, 4H), 1.08–1.08 (d, *J* = 13.4 Hz, 16H), 0.78–0.73 (t, *J* = 6.9 Hz, 6H), 0.68 (s, 4H). ^{13}C NMR (400 MHz, Methanol-*d*₄) δ 151.64, 142.60, 140.61, 139.13, 131.07, 130.44, 129.81, 129.31, 128.92, 127.37, 125.92, 121.04, 120.11, 55.26, 50.61, 50.35, 48.27, 48.06, 47.85, 47.63, 47.42, 47.21, 47.00, 39.93, 31.41, 29.40, 28.74, 28.68, 23.44, 22.23, 13.02. MS (Madi-Tof): calcd 1072.488, found $[\text{M}-2\text{H}-2\text{PF}_6]^{+}$ 780.598.

The methods for preparing **2b** are the same. Yield: 52.4%. The proton NMR spectrum of **2b** is shown in Figure S12. ^1H NMR (400 MHz, DMSO-*d*₆) δ 9.71 (s, 4H), 8.20–8.15 (d, *J* = 7.9 Hz, 2H), 8.07–8.02 (d, *J* = 7.6 Hz, 2H), 7.81–7.75 (d, *J* = 9.6 Hz, 2H), 7.52 (s, 2H), 7.50 (s, 4H), 7.50 (s, 4H), 7.48 (s, 2H), 7.44–7.40 (m, 2H), 7.40–7.39 (m, 2H), 7.38 (s, 2H), 7.37 (s, 2H), 7.17–7.12 (t, *J* = 7.9 Hz, 2H), 6.82 (s, 2H), 6.74–6.69 (d, *J* = 7.6 Hz, 2H), 4.16–3.97 (d, *J* = 9.7 Hz, 8H). ^{13}C NMR (400 MHz, DMSO-*d*₆) δ 150.05, 148.36, 141.83, 140.44, 139.81, 132.95, 132.37, 131.46, 131.24, 130.59, 129.29, 129.01, 128.67, 128.61, 127.48, 127.07, 124.05, 121.96, 121.63, 121.22, 66.08, 49.98, 49.68. MS (Madi-Tof): calcd 998.284, found $[\text{M}-2\text{H}-2\text{PF}_6]^{+}$ 705.716.

Acknowledgments

The project was supported by the National Natural Science Foundation of China (51273092), Natural Science Foundation of Jiangsu Province (BM2012010), the Six Peak Talents Foundation of Jiangsu Province (XCL-CXTD-009), NUPT under Grant NY217078, 03030XJ18008 and the Priority Academic Program Development of Jiangsu Higher Education Institutions, PAPD.

Disclosure statement

No potential conflict of interest was reported by the authors.

Funding

The project was supported by the National Natural Science Foundation of China [51273092], Natural Science Foundation of Jiangsu Province [BM2012010], the Natural Science Foundation of the Education Committee of Jiangsu Province, China [18KJA510003], the Six Peak Talents Foundation of Jiangsu Province [XCL-CXTD-009], NUPT under Grant [NY217078], [03030XJ18008] and the Priority Academic Program Development of Jiangsu Higher Education Institutions, PAPD.

References

- (1) Song, Z.Y.; Han, Z.Y.; Lv, S.X.; Chen, C.Y.; Chen, L.; Yin, L. C.; Cheng, J.J. *Chem. Soc. Rev.* **2017**, *46*, 6570–6599. DOI: [10.1039/c7cs00460e](https://doi.org/10.1039/c7cs00460e).
- (2) Goor, O.J.; Hendrikse, S.I.; Dankers, P.Y.; Meijer, E.W. *Chem. Soc. Rev.* **2017**, *46*, 6621–6637. DOI: [10.1039/c7cs00564d](https://doi.org/10.1039/c7cs00564d).
- (3) Lu, W.; Le, X.X.; Zhang, J.W.; Huang, Y.J.; Chen, T. *Chem. Soc. Rev.* **2017**, *46*, 1284–1294. DOI: [10.1039/c6cs00754f](https://doi.org/10.1039/c6cs00754f).
- (4) Bhattacharya, S.; Samanta, S.K. *Chem. Rev.* **2016**, *116*, 11967–12028. DOI: [10.1021/acs.chemrev.6b00221](https://doi.org/10.1021/acs.chemrev.6b00221).
- (5) Krieg, E.; Bastings, M.M.; Besenius, P.; Rybtchinski, B. *Chem. Rev.* **2016**, *116*, 2414–2477. DOI: [10.1021/acs.chemrev.5b00369](https://doi.org/10.1021/acs.chemrev.5b00369).
- (6) Voorhaar, L.; Hoogenboom, R. *Chem. Soc. Rev.* **2016**, *45*, 4013–4031. DOI: [10.1039/c6cs00130k](https://doi.org/10.1039/c6cs00130k).
- (7) Xiao, T.; Zhong, W.; Zhou, L.; Xu, L.; Sun, X.Q.; Elmes, R. B.; Wang, L. *Chin. Chem. Lett.* **2019**, *30*, 31–36. DOI: [10.1016/j.ccllet.2018.05.034](https://doi.org/10.1016/j.ccllet.2018.05.034).
- (8) Yang, L.L.; Tan, X.X.; Wang, Z.Q.; Zhang, X. *Chem. Rev.* **2015**, *115*, 7196–7239. DOI: [10.1021/cr500633b](https://doi.org/10.1021/cr500633b).
- (9) Wang, Q.; Cheng, M.; Jiang, J.L.; Wang, L.Y. *Chin. Chem. Lett.* **2017**, *28*, 793–797. DOI: [10.1016/j.ccllet.2017.02.008](https://doi.org/10.1016/j.ccllet.2017.02.008).
- (10) Wang, H.; Ji, X.F.; Li, Z.T.; Huang, F.H. *Adv. Mater.* **2017**, *29*, 1606117. DOI: [10.1002/adma.201700681](https://doi.org/10.1002/adma.201700681).
- (11) Bai, H.T.; Zhang, H.Y.; Hu, R.; Chen, H.; Lv, F.T.; Liu, L.B.; Wang, S. *Langmuir.* **2017**, *33*, 1116–1120. DOI: [10.1021/acs.langmuir.6b04469](https://doi.org/10.1021/acs.langmuir.6b04469).
- (12) Xu, D.F.; Liu, X.L.; Lu, R.; Xue, P.C.; Zhang, X.F.; Zhou, H.P.; Jia, J.H. *Org. Biomol. Chem.* **2011**, *9*, 1523–1528. DOI: [10.1039/c0ob00786b](https://doi.org/10.1039/c0ob00786b).
- (13) Lazzaroni, R.; Evans, R.C.; Maes, W.; Dubois, P.; Clement, S. *Macromol. Chem. Phys.* **2016**, *217*, 445–458. DOI: [10.1002/macp.201500280](https://doi.org/10.1002/macp.201500280).
- (14) Lin, J.Y.; Liu, B.; Yu, M.N.; Wang, X.H.; Bai, L.B.; Han, Y.M.; Ou, C.J.; Xie, L.H.; Liu, F.; Zhu, W.S.; Zhang, X.W.; Ling, H.F.; Stavrinou, P.N.; Wang, J.P.; Bradley, D.D.; Huang, W. *J. Mater. Chem. C.* **2018**, *6*, 1535–1542. DOI: [10.1039/C7TC04833E](https://doi.org/10.1039/C7TC04833E).
- (15) Xiong, C.X.; Sun, R.Y. *Chinese. J. Chem.* **2017**, *35*, 1669–1672. DOI: [10.1002/cjoc.201700229](https://doi.org/10.1002/cjoc.201700229).
- (16) Chen, J.W.; Huang, C.C.; Chao, C.Y. *ACS Appl. Mater. Interfaces.* **2014**, *6*, 6757–6764. DOI: [10.1021/am500518c](https://doi.org/10.1021/am500518c).
- (17) Lin, J.Y.; Wong, J.I.; Xie, L.H.; Dong, X.C.; Yang, H.Y.; Huang, W. *Macromol. Rapid Commun.* **2014**, *35*, 895–900. DOI: [10.1002/marc.201300831](https://doi.org/10.1002/marc.201300831).
- (18) Ni, X.L.; Chen, S.; Yang, Y.; Tao, Z. *J. Am. Chem. Soc.* **2016**, *138*, 6177–6183. DOI: [10.1021/jacs.6b01223](https://doi.org/10.1021/jacs.6b01223).

- (19) Kardelis, V.; Li, K.; Nierengarten, I.; Holler, M.; Nierengarten, J.F.; Adronov, A. *Macromolecules*. **2017**, *50*, 9144–9150. DOI: [10.1021/acs.macromol.7b02399](https://doi.org/10.1021/acs.macromol.7b02399).
- (20) Peurifoy, S.R.; Guzman, C.X. *Polym. Chem.* **2015**, *6*, 5529–5539. DOI: [10.1039/C5PY00420A](https://doi.org/10.1039/C5PY00420A).
- (21) Ji, X.F.; Yao, Y.; Li, J.Y.; Yan, X.Z.; Huang, F.H. *J. Am. Chem. Soc.* **2013**, *135*, 74–77. DOI: [10.1021/ja3108559](https://doi.org/10.1021/ja3108559).
- (22) Bai, W.; Wang, Z.; Tong, J.; Mei, J.; Qin, A.; Sun, J.Z.; Tang, B.Z. *Chem. Commun.* **2015**, *51*, 1089–1091. DOI: [10.1039/C4CC06510G](https://doi.org/10.1039/C4CC06510G).
- (23) Zhang, J.; Dong, S.; Zhang, K.; Liang, A.H.; Yang, X.Y.; Huang, F.; Cao, Y. *Chem. Commun.* **2014**, *50*, 8227–8230. DOI: [10.1039/c4cc03080j](https://doi.org/10.1039/c4cc03080j).
- (24) Zhang, J.; Zhang, K.; Huang, X.L.; Cai, W.Z.; Zhou, C.; Liu, S.J.; Huang, F.; Cao, Y. *J. Mater. Chem.* **2012**, *22*, 12759–12766. DOI: [10.1039/c2jm31773g](https://doi.org/10.1039/c2jm31773g).
- (25) Liang, A.H.; Huang, G.; Wang, Z.P.; Chen, S.L.; Hou, H.Q. *Prog. Chem.* **2016**, *28*, 471–481.
- (26) Abbel, R.; Schenning, A.P.; Meijer, E.W. *J. Polym. Sci. A*. **2009**, *47*, 4215–4233. DOI: [10.1002/pola.23499](https://doi.org/10.1002/pola.23499).
- (27) Yu, W.L.; Pei, J.; Huang, W.; Heeger, A.J. *Adv. Mater.* **2000**, *12*, 828–831. DOI: [10.1002/\(SICI\)1521-4095-\(200006\)12:11<828::AID-ADMA828>3.0.CO;2-H](https://doi.org/10.1002/(SICI)1521-4095-(200006)12:11<828::AID-ADMA828>3.0.CO;2-H).
- (28) Liang, J.; Qian, Y.; Xie, L.H.; Shi, N.E.; Chen, S.F.; Deng, X. Y.; Huang, W. *Acta Phys. Chim. Sin.* **2010**, *26*, 946–963.
- (29) Xie, L.H.; Zhu, R.; Qian, Y.; Liu, R.R.; Chen, S.F.; Lin, J.; Huang, W. *J. Phys. Chem. Lett.* **2010**, *1*, 272–276. DOI: [10.1021/jz900105v](https://doi.org/10.1021/jz900105v).
- (30) Yu, M.N.; Ou, C.J.; Liu, B.; Lin, D.Q.; Liu, Y.Y.; Xue, W.; Lin, Z.Q.; Lin, J.Y.; Qian, Y.; Wang, S.S.; Cao, H.T.; Bian, L. Y.; Xie, L.H.; Huang, W. *Chinese. J. Polym. Sci.* **2017**, *35*, 155–170. DOI: [10.1007/s10118-017-1897-6](https://doi.org/10.1007/s10118-017-1897-6).
- (31) Ou, C.J.; Ren, B.Y.; Li, J.W.; Lin, D.Q.; Zhong, C.; Xie, L.H.; Zhao, J.F.; Mi, B.X.; Cao, H.T.; Huang, W. *Org. Electron.* **2017**, *43*, 87–95. DOI: [10.1016/j.orgel.2016.12.029](https://doi.org/10.1016/j.orgel.2016.12.029).
- (32) Ashton, P.R.; Campbell, P.J.; Chrystal, E.J.; Glink, P.T.; Menzer, S.; Philp, D.; Spencer, N.; Stoddart, J.F.; Tasker, P.A.; Williams, D.J. *Angew. Chem. Int. Ed.* **1995**, *34*, 1865–1869. DOI: [10.1002/anie.199518651](https://doi.org/10.1002/anie.199518651).
- (33) Yamaguchi, N.; Gibson, H.W. *Angew. Chem. Int. Ed.* **1999**, *38*, 143–147. DOI: [10.1002/\(SICI\)1521-3773-\(19990115\)38:1/2<143::AID-ANIE143>3.0.CO;2-Y](https://doi.org/10.1002/(SICI)1521-3773-(19990115)38:1/2<143::AID-ANIE143>3.0.CO;2-Y).
- (34) Zhang, J.; Zhang, K.; Liu, S.; Liang, A.; Huang, X.; Huang, F.; Peng, J.; Cao, Y. *RSC Adv.* **2013**, *3*, 3829–3835. DOI: [10.1039/c3ra40249e](https://doi.org/10.1039/c3ra40249e).
- (35) Wang, F.; Han, C.; He, C.; Zhou, Q.; Zhang, J.; Wang, C.; Li, N.; Huang, F. *J. Am. Chem. Soc.* **2008**, *130*, 11254–11255. DOI: [10.1021/ja8035465](https://doi.org/10.1021/ja8035465).
- (36) Niu, Z.; Huang, F.; Gibson, H.W. *J. Am. Chem. Soc.* **2011**, *133*, 2836–2839. DOI: [10.1021/ja110384v](https://doi.org/10.1021/ja110384v).
- (37) De, G.T.; Smulders, M.M.; Wolffs, M.; Schenning, A.P.; Sijbesma, R.P.; Meijer, E.W. *Chem. Rev.* **2009**, *109*, 5687–5754. DOI: [10.1021/cr900181u](https://doi.org/10.1021/cr900181u).
- (38) Ohga, K.; Takashima, Y.; Takahashi, H.; Kawaguchi, Y.; Yamaguchi, H.; Harada, A. *Macromolecules*. **2005**, *38*, 5897–5904. DOI: [10.1021/ma0508606](https://doi.org/10.1021/ma0508606).
- (39) Abbel, R.; Grenier, C.; Pouderoijen, M.J.; Stouwdam, J.W.; Leclere, P.E.; Sijbesma, R.P.; Meijer, E.W.; Schenning, A.P. *J. Am. Chem. Soc.* **2009**, *131*, 833–843. DOI: [10.1021/ja807996y](https://doi.org/10.1021/ja807996y).
- (40) Yu, M.; Ou, C.; Liu, B.; Lin, D.; Liu, Y.; Xue, W.; Lin, Z.; Lin, J.; Qian, Y.; Wang, S.; Cao, H.; Bian, L.; Xie, L.; Huang, W. *Chinese. J. Polym. Sci.* **2017**, *35*, 155–170. DOI: [10.1007/s10118-017-1897-6](https://doi.org/10.1007/s10118-017-1897-6).
- (41) Kreyenschmidt, M.; Klaerner, G.; Fuhrer, T.; Ashenurst, J.; Karg, S.; Chen, W.D.; Lee, V.Y.; Scott, J. C.; Miller, R.D. *Macromolecules*. **1998**, *31*, 1099–1103. DOI: [10.1021/ma970914e](https://doi.org/10.1021/ma970914e).
- (42) Bliznyuk, V.N.; Carter, S.A.; Scott, J.C.; Klarner, G.; Miller, R.D.; Miller, D.C. *Macromolecules*. **1999**, *32*, 361–369. DOI: [10.1021/ma9808979](https://doi.org/10.1021/ma9808979).
- (43) Lee, J.I.; Klaerner, G.; Miller, R.D. *Chem. Mater.* **1999**, *11*, 1083–1088. DOI: [10.1021/cm981049v](https://doi.org/10.1021/cm981049v).
- (44) Jenekhe, S.A.; Osaheni, J.A. *Science*. **1994**, *265*, 765–768. DOI: [10.1126/science.265.5173.765](https://doi.org/10.1126/science.265.5173.765).
- (45) Osaki, H.; Chou, C.M.; Taki, M.; Welke, K.; Yokogawa, D.; Irlle, S.; Sato, Y.; Higashiyama, T.; Saito, S.; Fukazawa, A.; Yamaguchi, S. *Angew. Chem. Int. Ed.* **2016**, *55*, 7131–7135. DOI: [10.1002/anie.201602239](https://doi.org/10.1002/anie.201602239).
- (46) Vollbrecht, J.; *New J. Chem.* **2018**, *42*, 11249–11254. DOI: [10.1039/C8NJ02135J](https://doi.org/10.1039/C8NJ02135J).
- (47) Iida, A.; Yamaguchi, S. *Chem. Commun.* **2009**, *21*, 3002–3004. DOI: [10.1039/b901794a](https://doi.org/10.1039/b901794a).
- (48) Li, D.D.; Zhang, Y.P.; Fan, Z.Y.; Chen, J.; Yu, J.H. *Chem. Sci.* **2015**, *6*, 6097–6101. DOI: [10.1039/c5sc02044a](https://doi.org/10.1039/c5sc02044a).
- (49) Ma, X.F.; Sun, R.; Cheng, J.H.; Liu, J.Y.; Gou, F.; Xiang, H. F.; Zhou, X.G. *J. Chem. Educ.* **2016**, *93*, 345–350. DOI: [10.1021/acs.jchemed.5b00483](https://doi.org/10.1021/acs.jchemed.5b00483).
- (50) Zhang, X.; Huang, X.D.; Gan, X.P.; Wu, Z.C.; Yu, J.H.; Zhou, H.P.; Tian, Y.P.; Wu, J.Y. *Sens. Actuators B.* **2017**, *243*, 421–428. DOI: [10.1016/j.snb.2016.11.161](https://doi.org/10.1016/j.snb.2016.11.161).
- (51) Ranger, M.; Rondeau, D.; Leclerc, M. *Macromolecules*. **1997**, *30*, 7686–7691. DOI: [10.1021/ma970920a](https://doi.org/10.1021/ma970920a).
- (52) Tang, S.; Liu, M.; Gu, C.; Zhao, Y.; Lu, P.; Lu, D.; Ma, Y. *J. Org. Chem.* **2008**, *73*, 4212–4218. DOI: [10.1021/jo8006094](https://doi.org/10.1021/jo8006094).